Model of multifragmentation, equation of state, and phase transition

C. B. Das,[1] S. Das Gupta,[1] and A. Z. Mekjian[2]

[1]*Physics Department, McGill University, Montréal, Canada H3A 2T8*
[2]*Department of Physics and Astronomy, Rutgers University, Piscataway, New Jersey 08855, USA*

We consider a soluble model of multifragmentation which is similar in spirit to many models that have been used to fit intermediate energy heavy-ion collision data. We draw a p-V diagram for the model and compare with a p-V diagram obtained from a mean-field theory. We investigate the question of chemical instability in the multifragmentation model. Phase transitions in the model are discussed.

I. INTRODUCTION

Statistical models of multifragmentation have long been used to explain data from heavy-ion collisions. Such a model was first invoked for Bevalac results [1,2], and similar physical ideas, but with many substantial variations, were subsequently used for intermediate energy heavy-ion collisions [3–5]. In this work we consider a model of multifragmentation, variations of which have found many applications in the literature [6–11,13]. Thermodynamic properties of a simpler version of this model have also been discussed [15–17]. The model we use here has two kinds of particles but no Coulomb interaction. Throughout the rest of this paper we will refer to this model as the thermodynamic model. Typically, the number of particles in our model is 200, although we also use systems containing as many as 1000 particles. While we could have easily included a Coulomb interaction term, our objective here is different. The aim here is to test if because of two kinds of particles two features that have been discussed widely in recent literature (from studies in mean-field theory) persist in the thermodynamic model. These features are chemical instability (analogous to mechanical instability) and first order transition turning into second order. We therefore need to highlight some features that are present both in the thermodynamic model and in mean-field theories when mean field theories are applied to intermediate energy heavy ion physics. Typically, mean-field theories use homogeneous infinite matter (hence no surface energy terms) and no Coulomb interaction. Finite systems with Coulomb and surface terms have also been included [14] in mean-field models, but this makes discussions more complicated and we want to stay at the simplest level. As shown in Ref. [6], surface energy terms play an important role in a thermodynamic model and are included. Moreover, since we will concentrate on two component systems, symmetry energy terms are included as they are also in mean-field theories.

II. THE THERMODYNAMIC MODEL

The thermodynamic model has been described in many places [6,7,11]. For completeness and to enumerate the parameters we provide some details.

Assume that the system that breaks up after two ions hit each other can be described as a hot equilibrated nuclear system characterized by a temperature T and a freeze-out volume V within which there are A nucleons ($A=Z+N$). The partition function of the system is given by

$$Q_{Z,N} = \sum \prod_{i,j} \frac{\omega_{i,j}^{n_{i,j}}}{n_{i,j}!}. \qquad (2.1)$$

Here $n_{i,j}$ is the number of composites with proton number i and neutron number j and $\omega_{i,j}$ is the partition function of a single composite with proton, neutron numbers i,j, respectively. The sum is over all partitions of Z,N into clusters and nucleons subject to two constraints: $\Sigma_{i,j} i n_{i,j} = Z$ and $\Sigma_{i,j} j n_{i,j} = N$. These constraints would appear to make the computation of $Q_{Z,N}$ prohibitively difficult, but a recursion relation exists which allows the computation of $Q_{Z,N}$ quite easy on the computer even for large Z or N [12]. Three equivalent recursion relations exist, any one of which could be used. For example, one such relation is

$$Q_{z,n} = \frac{1}{z} \sum_{i,j} i \omega_{i,j} Q_{z-i,n-j}. \qquad (2.2)$$

The average number of particles of the species i,j is given by

$$\langle n_{i,j} \rangle = \omega_{i,j} \frac{Q_{Z-i,N-j}}{Q_{Z,N}}. \qquad (2.3)$$

All nuclear properties are contained in $\omega_{i,j}$. It is given by

$$\omega_{i,j} = \frac{V_f}{h^3} [2\pi(i+j)mT]^{3/2} \times q_{i,j,int}. \qquad (2.4)$$

Here V_f is the free volume within which the particles move; V_f is related to V through $V_f = V - V_{ex}$, where V_{ex} is the excluded volume due to finite sizes of composites. This is the only interaction between clusters we try to simulate. Thus the thermodynamic model is not an exact description of the system considered here but another approximation to it which has some interesting features that we hope to show. This restricts the validity of the model to low density (i.e., large V). Further, we take V_{ex} to be fixed, independent of multiplicity. In reality, V_{ex} should depend upon multiplicity [18]. We take it to be constant and equal to $V_0 = A/\rho_0$, where ρ_0 is the normal nuclear density and A is the number of nucleons

of the disassembling system. As in previous applications, we restrict the model to freeze-out densities less than $\rho/\rho_0 = 0.5$, that is, $V \geqslant 2V_0$. The factor $q_{i,j,int}$ is the internal partition function of the composite. Define $a = i + j$. Then

$$q_{i,j,int} = \exp\left[Wa - \sigma a^{2/3} - s\frac{(i-j)^2}{a} + aT^2/\epsilon_0\right]\Bigg/ T. \tag{2.5}$$

Here $W = 15.8$ MeV, $\sigma = 18$ MeV, $s = 23.5$ MeV, and $\epsilon = 16.0$ MeV. The reader will recognize the volume, surface, and symmetry energy of the cluster i,j and the contribution to the internal partition function from excited states in the Fermi-gas formulation. For $a(=i+j) \geqslant 5$ we use this formula. For lower masses we simulate no Coulomb case by setting the binding energy of ^{3}He equal to the binding energy of ^{3}H and binding energy of ^{4}Li equal to the binding energy of ^{4}H. In the weight of Eq. (2.4) we have not included a Fisher droplet model τ which is a power law prefactor that is important around the critical point. Away from a critical point, exponential terms dominant the weight and this is the region we study in this paper. Such a term can be included, but our main focus is on the role of the symmetry energy in two component systems and related questions of chemical instability.

For a given a, what are the limits on i (or $j = a - i$)? This is a nontrivial question. In the results we will show, we have taken limits by calculating the drip lines of protons and neutrons as given by the above binding energy formula. Limiting oneself within the drip lines is a well-defined prescription, but is likely to be an underestimation since resonances show up in particle-particle correlation experiments. On the other hand, for a given a, taking the limits of i from 0 to a is definitely an overestimation.

There is another consideration that restricts the validity of the model. We have assumed [Eq. (2.1)] that the standard correction $n_{i,j}!$ takes care of antisymmetry or symmetry of the particles. In the range $T > 3$ MeV and $\rho/\rho_0 < 0.5$ this is usually true. At low temperatures where one might apprehend the usual correction to fail, it survives because many composites appear, thus there is not enough of any particular species to make (anti)symmetrization an important issue. At much higher temperature the number of protons and neutrons increase but as is well known, the $n!$ correction takes the approximate partition function towards the proper one at high temperature. We define $y \equiv Z/(Z+N)$, where Z and N are the total proton and neutron numbers of the disintegrating system and the theory works even at low temperatures if y is in the vicinity of 0.5. But, for example, at $T = 5.0$ MeV and $y = 0$ (neutron matter), this is a terrible model. Now the number of neutrons is large and the temperature is not high and Fermi-Dirac statistics must be enforced. This was studied quantitatively in Ref. [19]. In our applications of the thermodynamic model we will confine y to be between 0.3 and 0.7 and $T \geqslant 3$ MeV. This is indeed not very restrictive since this encompasses the drip lines and so the model, which was devised for intermediate energy heavy-ion collisions, will be applicable. For ^{124}Sn $+ ^{124}$Sn collisions, a much studied case, the value of y is 0.4.

By equation of state (EOS) we mean $p - V$ diagrams for fixed temperatures. This can be obtained by exploiting the equation $p = T(\partial \ln Q_{Z,N}/\partial V_f)$. From Eqs. (2.1) and (2.3), this reduces to $p = (T/V_f)(\Sigma\langle n_{i,j}\rangle - 1)$, where -1 within the parentheses corrects for center of mass motion. The simplicity of this formula suggests that we just have a noninteracting gas with many species with V being replaced by V_f. But this is deceptive. In fact, $\Sigma\langle n_{i,j}\rangle$ (which is the multiplicity) is not fixed but varies as a function of both temperature T and volume V, thus this is not anything as simple as a mixture of noninteracting species. It is indeed interactions that make or break clusters to produce the final equilibrium or statistical distribution of fragments. In this sense interactions are also included.

Since ours is a canonical model, we do not need the chemical potentials μ_p (proton chemical potential) and μ_n, but we compute them anyway from the relation $\mu = (\partial F/\partial n)_{V,T}$. We know the values of $Q_{Z,N}, Q_{Z-1,N}$, and $Q_{Z,N-1}$. Since F is just $-T \ln Q$, we compute μ_p from $\mu_p = -T(\ln Q_{Z,N} - \ln Q_{Z-1,N})$ and μ_n from $-T(\ln Q_{Z,N} - \ln Q_{Z,N-1})$. Indeed, the grand canonical version of the thermodynamic model we are solving has been known for a long time in heavy ion collision physics [2]. There the μ_p and μ_n arise naturally. We have checked that the grand canonical values of μ_p and μ_n are indeed very close to the ones we derive by exploiting the canonical partition functions whose values we know numerically. Throughout this work, whenever we plot μ's we have obtained the values from a canonical calculation. One might think that since our model has many species there should be many μ's, but, in fact, all μ's can be expressed in terms of only μ_p and μ_n. Since our model is based solely on phase space, chemical equilibrium is, in fact, implied.

III. A MEAN-FIELD MODEL

We want to contrast the model above with mean-field theories. Our mean-field calculation uses the simplest model consistent with nuclear matter binding energy, saturation density, compressibility, and symmetry energy for asymmetric matter. The potential energy density is taken to be

$$V(\rho_n, \rho_p) = \frac{A_u}{\rho_0}\rho_n\rho_p + \frac{A_l}{2\rho_0}(\rho_n^2 + \rho_p^2) + \frac{B}{\sigma+1}\frac{\rho^{\sigma+1}}{\rho_0^\sigma}. \tag{3.1}$$

Here $\rho_0 = 0.16$ fm^{-3} and ρ_n and ρ_p are neutron and proton densities and $\rho = \rho_n + \rho_p$. The dimensionless constant σ and A_u, A_l, B (all in MeV) are chosen to reproduce nuclear matter binding at 16 MeV per particle, saturation density at 0.16 fm^{-3}, compressibility at 201 MeV, and symmetry energy at 23.5 MeV. The energy per particle (including kinetic energy) at $T = 0$ is

$$E/A = A_u \frac{\rho_n\rho_p}{\rho\rho_0} + \frac{A_l}{2\rho\rho_0}(\rho_n^2 + \rho_p^2) + \frac{B}{\sigma+1}\left(\frac{\rho}{\rho_0}\right)^\sigma$$

$$+ 22.135 \times \left[\frac{\rho_p}{\rho}\left(\frac{2\rho_p}{\rho_0}\right)^{2/3} + \frac{\rho_n}{\rho}\left(\frac{2\rho_n}{\rho_0}\right)^{2/3}\right]. \tag{3.2}$$
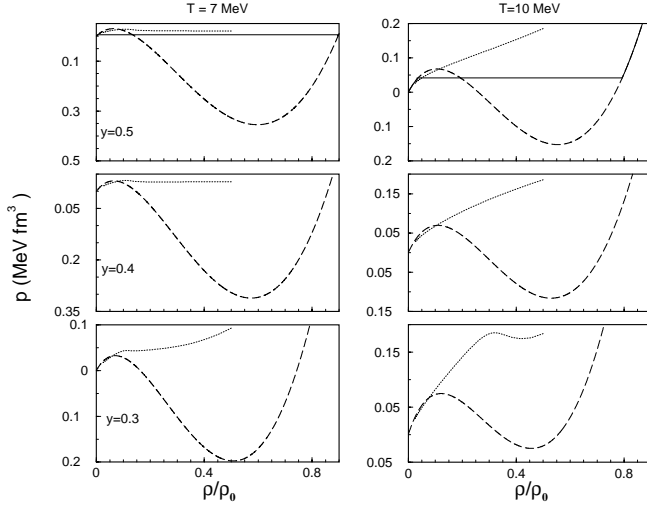
FIG. 1. The EOS in the thermodynamic model at different temperatures 7 and 10 MeV (left and right panels, respectively) and with different proton fractions. The dotted lines represent the EOS in the thermodynamic model. The dashed lines are the straightforward EOS in the mean-field model. For $y = 0.5$ a Maxwell construction is also done in the mean-field model (solid line). For the cases $y = 0.4$ and $y = 0.3$, the coexistence line in a mean-field theory is no longer horizontal but has a slope with the liquid endpoint at a somewhat higher pressure than the gas endpoint, as shown in Refs. [21,22].

The values of the constants are: $\sigma = 7/6$, $A_u = -379.2$ MeV, $A_l = -334.4$ MeV, and $B = 303.9$ MeV.

The Hartree-Fock energy of an orbital is given by

$$\epsilon = p^2/2m + A_u(\rho_u/\rho_0) + A_l(\rho_l/\rho_0) + B(\rho/\rho_0)^\sigma. \quad (3.3)$$

The value of μ_p is found by solving for a given ρ_p and $\beta = 1/T$,

$$\rho_p = \frac{8\pi}{h^3} \int_0^\infty \frac{p^2 dp}{\exp[\beta(\epsilon_p - \mu_p)] + 1}. \quad (3.4)$$

Similarly μ_n is extracted from ρ_n. The pressure has contributions from kinetic energy and potential energy. The contribution from kinetic energy is calculated from well-known Fermi-gas model formula. Contribution to pressure from interaction is

$$p_{Skyrme} = \frac{A_u}{\rho_0}\rho_n\rho_p + \frac{A_l}{2\rho_0}[(\rho_n)^2 + (\rho_p)^2] + \frac{\sigma}{\sigma+1}B\left(\frac{\rho}{\rho_0}\right)^\sigma \rho. \quad (3.5)$$

IV. EOS IN THE THERMODYNAMIC MODEL

Figure 1 shows the p-ρ diagrams at constant temperature for the thermodynamic model. We restrict the value of $y = \rho_p/(\rho_p + \rho_n)$ between 0.3 and 0.5 and ρ/ρ_0 between 0 and 0.5 because outside these ranges the validity of the thermodynamic model is significantly reduced. For the case $y = 0.5$ we also show the EOS obtained from the mean-field theory. Two curves are drawn for the mean-field model. One

is the straightforward p-ρ diagram, the other one is with Maxwell construction. We notice that without the Maxwell construction, the mean-field EOS is widely different from the one obtained from the thermodynamic model. The p-ρ diagram with Maxwell construction is much closer specially at temperature 7 MeV. The p-ρ diagrams at $T = 10$ MeV in the two models are not that close. At least part of the reason is that the thermodynamic model is drawn for exactly 200 nucleons but the mean-field theory uses a grand canonical ensemble and hence is applicable to infinite systems only. We have checked that for a system of 500 nucleons, the thermodynamic p-ρ diagram is closer to the Maxwell constructed p-ρ diagram. For $y = 0.3$ and $y = 0.4$ we have drawn merely the straightforward p-ρ diagram. In these cases, the coexistence line in a mean-field theory is no longer horizontal but has a slope with the liquid endpoint at a somewhat higher pressure than the gas endpoint as shown in Refs. [21,22].

We want to point out that regions of negative compressibility ($dp/d\rho < 0$) which are common in mean-field theory (Maxwell construction eliminates these) are almost absent in the thermodynamic model (they are present when plotted in an expanded scale, see Fig. 3) and one would be tempted to conclude that the thermodynamic model is a good lowest order approximation. The thermodynamic model includes all inhomogeneous distributions of matter from single nucleons and light clusters with gaslike behavior to very large liquidlike clusters. This feature approximates the Maxwell construction incorporated into a mean field theory which splits the system into two parts with liquid and gas densities. The very small region of negative compressibility left over has its origin probably in the finite particle number effect and is not an inherent error in the model. This is dealt with again in Sec. VII. Mean-field theory descriptions of two component systems introduce new features into the description not present in one component systems. Specifically, a new variable has to be introduced, such as the proton fraction y, which can be different in the two phases. The liquid phase can have one value of y, with the gas phase having another value, while still maintaining the total number of protons and neutrons. With a new variable, the coexistence curve and instability curve of one component systems become surfaces in p, T, and y for two components. In mean-field descriptions, the first order phase transition of one component systems becomes a second order phase transition in two component systems. Moreover, mechanical instability and chemical instability no longer coincide. We now turn our attention to features associated with chemical instability in our model.

V. ISOSPIN FRACTIONATION

Isospin fractionation is a well-established experimental phenomenon [20]. If the disintegrating system has a given $N/Z > 1$ then, after collision, the measured n_n/n_p ratio (where n_n, n_p are measured single neutron and proton yields, respectively) is higher than N/Z. Similarly, the ratio of measured $\langle n_{1,2}\rangle/\langle n_{2,1}\rangle$ is higher than what one might expect from the N/Z ratio of the disintegrating system. This then implies

that if there is a large chunk left after the breakup it must have a n/z ratio lower than original N/Z since the total number of neutrons and protons must be conserved. If we characterize n/z ratio, etc., in terms of the parameter y we have been using, then if y_{source} is less than 0.5, then y of the large chunk is greater than y_{source} and $\langle n_p \rangle/(\langle n_p \rangle + \langle n_n \rangle)$ is less than y_{source}.

A priori, it would seem difficult to get this aspect out of a mean-field model but in a seminal piece of work Muller and Serot have demonstrated how this might come about [21,22]. In mean-field theory, analogous to mechanical instability ($\partial p/\partial \rho < 0$) there appear regions of chemical instability, i.e., $\partial \mu_p/\partial y < 0$ (or $\partial \mu_n/\partial y > 0$), when two kinds of particles are involved. One can avoid this unphysical region of chemical instability but then needs to consider splitting the system into two parts, each homogeneous but distinct from the other, one belonging to the liquid phase with higher y value and the other to the gas phase with lower y value. One consequence of this is that the phase transition takes place neither at constant pressure nor at constant volume and what would have been a first order phase transition, becomes a second order phase transition.

In the thermodynamic model, isospin fractionation happens naturally. In general, the model has, as final products, all allowed composites, $a, b, c, d, \ldots$, where the composite labeled a has $y_a = i_a/(i_a + j_a)$, where i_a, j_a is the number of protons and number of neutrons, respectively, in the composite a. The only law of conservation is $Z = \Sigma_a i_a \times n_a$ and $N = \Sigma_a j_a \times n_a$. So a large chunk can exist with higher y than that of the whole system and populations of other species can adjust to obey overall conservation laws. Whatever partition lowers the free energy will happen. The thermodynamic model is dramatically different from mean-field models. The most significant difference is that, in the thermodynamic model, if we prescribe that dissociation takes place at $\rho/\rho_0 = 0.3$ we still have only clusters with normal nuclear density and properties and also nucleons. It is just that there are empty spaces between different clusters and nucleons in the region of dissociation. But in mean-field models $\rho/\rho_0 = 0.3$ will imply that the nuclear matter is uniformly stretched to this density. While this can happen as a transient phenomenon such as in transport calculation, whether this can also exist as an equilibrium situation is highly questionable.

An example of isospin fractionation in the thermodynamic model is shown in Fig. 2. The formalism developed in Sec. II can also be extended to calculate the average number of nucleons and protons (or neutrons) in the largest cluster. For brevity, we do not write the formulas here, but these are straightforward extensions of Eqs. (2.7) and (2.8) given in Ref. [6]. Figure 2 shows results from such a calculation. If y of the disintegrating system is less than 0.5, the y value of the largest cluster is larger than that of the source. Correspondingly, $(\langle n_p \rangle)/(\langle n_p \rangle + \langle n_n \rangle)$ is much smaller that y_{source}. (It should be mentioned that the number of protons and neutrons will be augmented from decays of hot composites, so what is plotted in Fig. 2 is not what will actually be observed in experiments). Further, the isospin fractionation happens whether the dissociation takes place at constant volume or constant pressure.
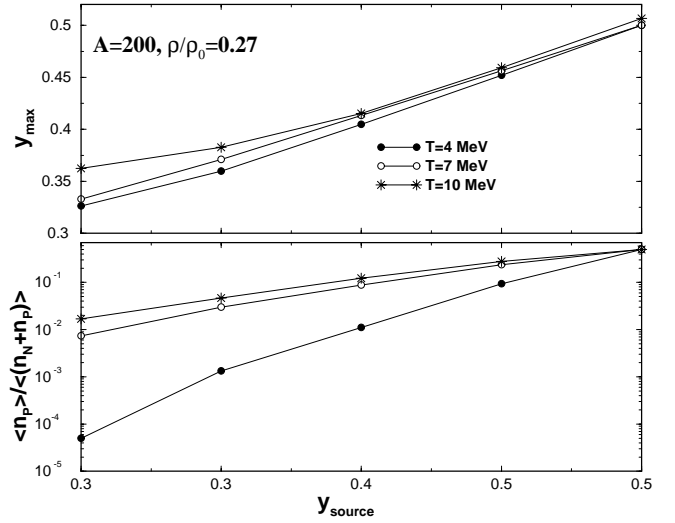

FIG. 2. Example of isospin fractionation in the thermodynamic model. y of the largest cluster (top panel) is plotted in the top panel. This y is larger than the y value of the whole system. The lower part of the figure shows that the gas of nucleons is very rich. For example, for $y = 0.4$ and $T = 7–10$ MeV, $\langle n_n \rangle \approx 10 \langle n_p \rangle$ while for $T = 4$ MeV, $\langle n_n \rangle \approx 100 \langle n_p \rangle$.

In this and many other aspects, the thermodynamic model is very similar to the lattice gas model (LGM) with isospin dependence. For an accurate solution of LGM one has to give up the mean-field approach and obtain results by Monte Carlo simulation. Here also many composites are produced with many different y values [23,24]. Isospin fractionation happens naturally [24].

VI. INSTABILITY IN THE THERMODYNAMIC MODEL

Figure 1 shows that compared to the mean-field model, regions of mechanical instability with $\partial p/\partial \rho < 0$ nearly disappear in the thermodynamic model. In an expanded scale, they are more readily seen (Fig. 3) where we have drawn p-ρ diagram for a constant temperature $T = 7.0$ MeV but different y's.

We clearly have some regions of mechanical instability. Chemical instability implies $(\partial \mu_p/\partial y)_{p,T} < 0$. We investigate that now. At $T = 7$ MeV, we have drawn μ_p (and μ_n) at four pressures (Fig. 4). To get an understanding of the behavior, we need to also look at Fig. 3. At the lowest pressure shown, $p = 0.02$ MeV fm^{-3} (Fig. 4), the horizontal constant pressure curve cuts the isothermals (Fig. 3) at the low density side only (between A and B) and μ_p rises monotonically between $y = 0.3$ and $y = 0.5$. The next constant pressure curve, at $p = 0.025$ MeV fm^{-3} (Fig. 4) cuts all isothermals (Fig. 3) at low density side ($\rho/\rho_0 < 0.1$) between C and D and a few isothermals at higher density side. Between C and D, y increases as does μ_p. The points marked D and E have the same values of p and T but very slightly differing values of μ_p. As we move to the right from E along the line $p = 0.025$ MeV fm^{-3} the value of y drops as also the value of μ_p. We forego describing graphs at other pressures but the figure shows there is a very small region where $\partial \mu_p/\partial \rho$ is
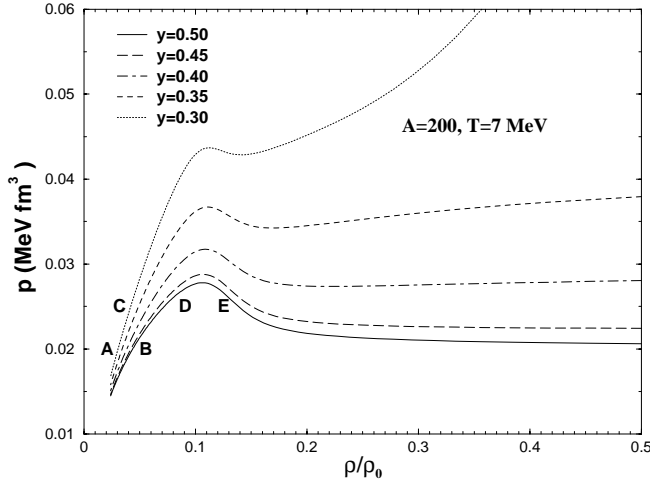
FIG. 3. EOS (p-ρ) in the thermodynamic model at $T = 7.0$ MeV, but for different y's.

negative (Fig. 4, $p = 0.035$ MeV fm^{-3}). The not so obvious feature is the appearance of two branches in both μ_p and μ_n (i.e., for example, the $p = 0.025$ MeV fm^{-3} curve). To discuss this in terms of simpler and well-known models we consider $y = 0.5$, the case for which there is only one $\mu = \mu_n = \mu_p$ [for a general y, one could consider $\mu = y\mu_p + (1-y)\mu_n$]. The behavior of μ at $y = 0.5$ and temperature $T = 7.0$ MeV as a function of ρ/ρ_0 as given in our model for 200 nucleons is shown in Fig. 5. The model is inappropriate at high density so we cut off ρ at ρ/ρ_0 at 0.5.

For the $y = 0.5$ curve we also depict schematically what the behavior would have been if we had a Maxwell-corrected Van der Waals fluid. From some point A, the chemical potential would remain unchanged (shown by a horizontal line ending at B which is the end point of our density). A more familiar plot is μ against pressure p for a fixed temperature. This is shown in the right panel for our model. For a Van der Waals fluid, the segment from A to B would simply collapse to the point A.
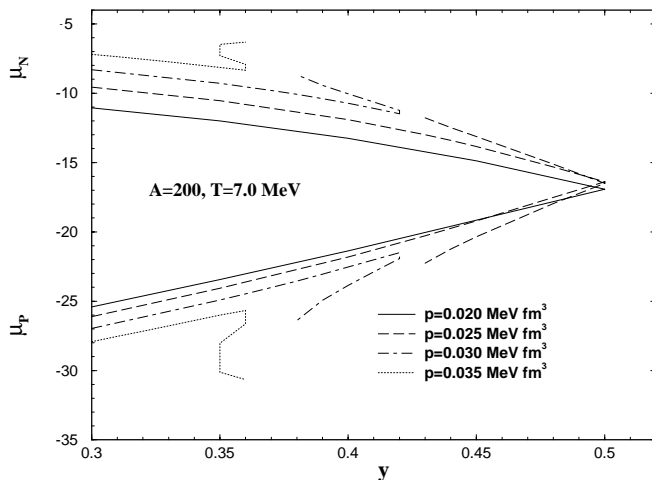

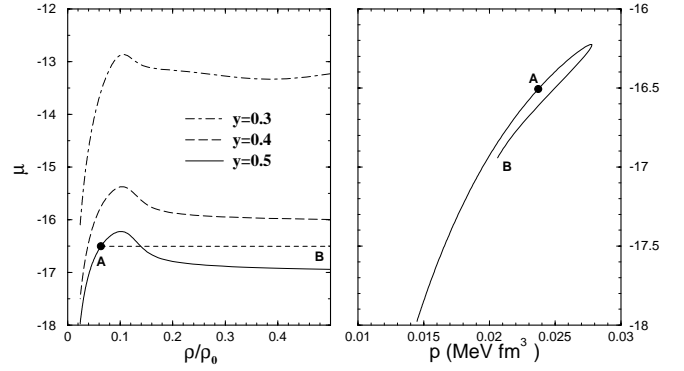FIG. 4. μ_P and μ_N as a function of y. Here $T = 7$ MeV.

FIG. 5. $\mu = y\mu_p + (1-y)\mu_n$ as a function of ρ/ρ_0 for different y's (left panel). For $y = 0.5$ $\mu = \mu_p = \mu_n$. The temperature is 7 MeV. In the right panel the behavior of μ is shown as a function of pressure p for $y = 0.5$ and $T = 7$ MeV.

VII. SPECIFIC HEATS IN THE MODEL

In Ref. [6] where the thermodynamic model was first studied for phase transitions, it was pointed out that for a given density ρ, the specific heat per particle C_V/A tends to ∞ at a particular temperature when the particle number A tends to ∞. Since $C_V = (\partial E/\partial T)_V = T(\partial S/\partial T)_V = -T(\partial^2 F/\partial^2 T)_V$, a singularity in C_V signifies a break in the first derivative of F, the free energy, and a first order phase transition. The model in Ref. [6] considered one kind of particle although binding energy, surface energy, etc., were chosen to mimic the nuclear case. We mention here that a similar model in the grand canonical ensemble predicted a large but finite C_V/A at boiling, although values are not quoted [15]. We hope to address this issue further in a later publication.

The growth of C_V/A with A is also seen in the case where we take into account two kinds of particles explicitly (Fig. 6,
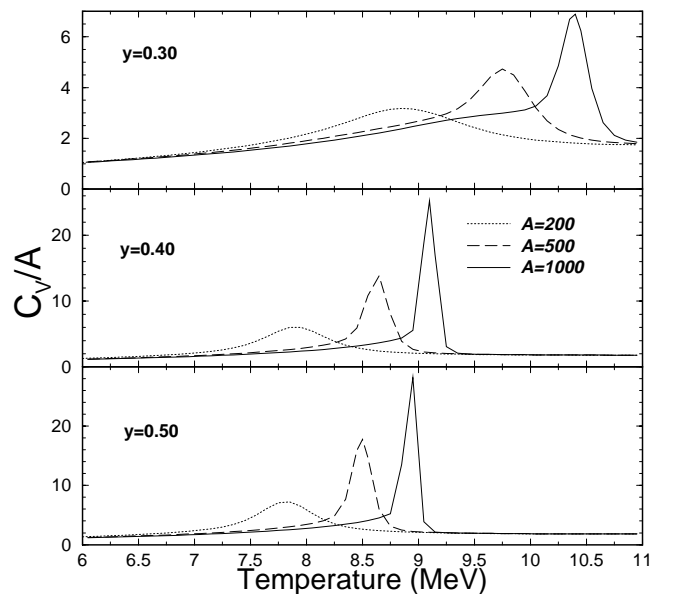

FIG. 6. C_V/A as a function of temperature for systems of 200, 500, and 1000 particles with different proton fractions.

see also Ref. [7]). The calculated C_V/A becomes progressively sharply peaked as A increases for all y values between 0.3 and 0.5. This behavior of the specific heat is very different from that of mean-field model of nuclear matter where the specific heat at constant volume varies smoothly from a low temperature Fermi gas to an ideal gas as T increases. In a thermodynamic model with fragmentation, this behavior is modified by the surface energies that arise in the multifragmentation of the original nucleus into clusters of different sizes. The peak in the specific heat occurs at the point where the largest cluster suddenly disappears. This behavior is nuclear boiling [25].

Specific heat per particle C_p/A in the model has not been considered before. We notice there are regions with $\partial p/\partial \rho < 0$ (even though these regions are much less visible than in the mean-field model). Their presence might indicate finite particle number effects or it may be a shortcoming of the model. Ongoing calculations suggest it is particle number effect rather than an inherent problem in the model. These negative regions of compressibility can lead to negative values of C_p. This is a contentious issue at the moment and we intend to deal with these issues fully in a future publication.

VIII. SUMMARY

We looked at several features of a thermodynamic model (which has seen many applications in data fitting) and a mean-field model. Equation of state in mean-field theory has large regions of mechanical instability even for infinite systems and one needs to do a Maxwell construction to eliminate these. By contrast, the thermodynamic model has directly an EOS that becomes very flat with density and volume and this behavior resembles a real system undergoing a first order phase transition. In mean-field models, when the system enters the region of instability, it fragments into pieces. This fragmentation is directly included in the thermodynamic model and this is the reason for relative flatness in the EOS. The cluster distribution readjusts itself with changes in V or ρ to maintain a nearly constant pressure. Isospin fractionation seen in experiments can be also obtained in the mean-field model but it requires a bifurcation in the isotopic space. It also requires that during dissociation neither pressure nor volume remain constant. By contrast, isospin fractionation occurs naturally in the thermodynamic model and can happen either at constant volume or at constant pressure. Large differences between these two models also appear in the calculation of C_V. The thermodynamic model has a strong peak in C_V whose origin are surface energy terms in the multifragmentation process which is lacking in a mean-field model of homogeneous nuclear matter. This peak is associated with the phenomenon of nuclear boiling and the sudden disappearance of the largest cluster.

[1] A.Z. Mekjian, Phys. Rev. Lett. **38**, 640 (1977).

[2] S. Das Gupta and A.Z. Mekjian, Phys. Rep. **72**, 131 (1981).

[3] J.P. Bondorf, A.S. Botvina, A.S. Iljinov, I.N. Mishustin, and K. Sneppen, Phys. Rep. **257**, 133 (1995).

[4] J. Randrup and S.E. Koonin, Nucl. Phys. **A471**, 355c (1987).

[5] D.H.E. Gross, Phys. Rep. **279**, 119 (1997).

[6] S. Das Gupta and A.Z. Mekjian, Phys. Rev. C **57**, 1361 (1998).

[7] P. Bhattacharyya, S. Das Gupta, and A.Z. Mekjian, Phys. Rev. C **60**, 054616 (1999).

[8] P. Bhattacharyya, S. Das Gupta, and A.Z. Mekjian, Phys. Rev. C **60**, 064625 (1999).

[9] S. Pratt and S. Das Gupta, Phys. Rev. C **62**, 044603 (2000).

[10] A. Majumder and S. Das Gupta, Phys. Rev. C **61**, 034603 (2000).

[11] S. Das Gupta, A.Z. Mekjian, and M.B. Tsang, Adv. Nucl. Phys. **26**, 91 (2001).

[12] K.C. Chase and A.Z. Mekjian, Phys. Rev. C **50**, 2078 (1994).

[13] M.B. Tsang *et al.*, Phys. Rev. C **64**, 054615 (2001).

[14] S.J. Lee and A.Z. Mekjian, Phys. Rev. C **63**, 044605 (2001).

[15] K.A. Bugaev, M.I. Gorenstein, I.N. Mishustin, and W. Greiner, Phys. Rev. C **62**, 044320 (2000).

[16] K.A. Bugaev, M.I. Gorenstein, I.N. Mishustin, and W. Greiner, Phys. Lett. B **498**, 144 (2001).

[17] J.B. Elliott and A.S. Hirsch, Phys. Rev. C **61**, 054605 (2001).

[18] A. Majumder and S. Das Gupta, Phys. Rev. C **59**, 845 (1999).

[19] B.K. Jennings and S. Das Gupta, Phys. Rev. C **62**, 014901 (2000).

[20] H.S. Xu *et al.*, Phys. Rev. Lett. **85**, 716 (2000).

[21] H. Muller and B.D. Serot, Phys. Rev. C **52**, 2072 (1995).

[22] H. Muller and B. D. Serot, in *Isospin Physics in Heavy-Ion Collisions at Intermediate Energy*, edited by B. A. Li and W. U. Schroder (Nova Science, Huntington, New York, 2001).

[23] J. Pan and S. Das Gupta, Phys. Rev. C **57**, 1839 (1998).

[24] Ph. Chomaz and F. Gulminelli, Phys. Lett. B **447**, 221 (1999).

[25] F. Reif, *Fundamentals of Statistical and Thermal Physics* (McGraw-Hill, New York, 1965), Chap. 8.